

CHARACTERIZATION OF THE DISTORTION OF OFDM/OQAM MODULATIONS UNDER FREQUENCY SELECTIVE CHANNELS

Xavier Mestre¹, Matilde Sánchez-Fernández², Antonio Pascual-Iserte³

¹Centre Tecnològic de Telecomunicacions de Catalunya, Barcelona (Spain)

²Universidad Carlos III de Madrid, Madrid (Spain)

³Universitat Politècnica de Catalunya, Barcelona (Spain)

e-mails: xavier.mestre@cttc.cat, mati@tsc.uc3m.es, antonio.pascual@upc.edu

ABSTRACT

Filterbank based multicarrier modulations are well known to perform poorly in frequency selective channels when single tap carrier-by-carrier equalization is used. This degradation is caused by the inherent distortion in terms of inter-symbol and inter-carrier interference at the receiving side, which cannot be compensated via single-tap equalization. We provide here an asymptotic characterization of this effect. More specifically, we derive the asymptotic distortion after a single-tap perfect equalizer under the assumption that the number of carriers is asymptotically large.

Index Terms— Filter-bank multi-carrier modulations, OFDM/OQAM, frequency-selective channel.

1. INTRODUCTION

Filterbank multicarrier (FBMC) modulations have been proposed as spectrally efficient alternatives to the classical orthogonal frequency-division multiplexing (OFDM) modulation. Two are the main advantages of FBMC modulations with respect to classical cyclic prefix based OFDM: on the one hand, they do not require the presence of a cyclic prefix; on the other, they naturally implement pulse shaping, which guarantees a well-localized spectral occupancy and prevents out-of-band emissions. These two features result in a much more efficient multicarrier modulation, which makes better use of the available spectral resources.

Unfortunately FBMC modulations present an important drawback that has traditionally prevented their widespread application in wireless scenarios, namely their lack of robustness against channel frequency selectivity [1]. It is well known that channel frequency selectivity generates inter-symbol and inter-carrier interference at the receiver, and this effect cannot be compensated by single tap carrier-by-carrier equalizers (as it is the case in traditional OFDM with cyclic prefix).

This paper has been financially supported by research grants TEC2008-06327-C03-01/02/03, TEC2011-29006-C03-01/02/03 and 2009SGR1046.

So far, a lot of research has been devoted to the study of specific equalization techniques for different filterbank multicarrier architectures, see e.g. [2, 3, 4] and references therein. However, little work has been carried out in order to characterize this distortion and to study its dependence on the FBMC system parameters, such as the prototype pulse shape or the channel frequency response. This characterization is important in order to predict the performance of the modulation in a practical frequency selective channels, and thereby establish the best modulation and coding scheme given a specific channel response. This paper tries to provide further insights along these lines by deriving a first-order asymptotic characterization of the mean squared error (MSE) caused by this distortion, assuming that a single tap carrier-by-carrier equalizer is used. The asymptotic expressions provide a valuable tool to characterize the dependence of the residual distortion on the different FBMC modulation parameters.

2. SIGNAL MODEL

We consider the discrete-time formulation of a filterbank multicarrier system using an OFDM/OQAM modulation [5] consisting of $2M$ carriers and real-valued prototype filter $p_M[k]$, $k = 1, \dots, N$, where N is the length of the prototype pulse, assumed even to simplify the exposition. We will assume that $p_M[k]$ presents even symmetry with respect to its central sample, namely $p_M[k] = p_M[N - k + 1]$, $k = 1, \dots, N$. We will denote by κ the length of the prototype pulse in number of multicarrier filters, namely $\kappa = N/(2M)$. Without loss of generality, we will assume that κ is an even natural number¹, and we will define a $2M \times \kappa$ matrix \mathbf{P} containing the prototype pulse samples arranged as

$$\mathbf{P} = \begin{bmatrix} p_M[1] & p_M[2M+1] & \cdots & p_M[2M(\kappa-1)+1] \\ p_M[2] & p_M[2M+2] & \cdots & p_M[2M(\kappa-1)+2] \\ \vdots & \vdots & \ddots & \vdots \\ p_M[2M] & p_M[4M] & \cdots & p_M[N] \end{bmatrix}. \quad (1)$$

¹Otherwise, simply add zeros at either side of $p_M[k]$ and redefine N .

Each of the rows of \mathbf{P} contains the impulse response of a different polyphase component of the prototype filter, whose transfer function will be denoted by $P_\ell(z)$, $\ell = 1 \dots 2M$, i.e. $P_\ell(z) = \sum_{n=0}^{\kappa-1} p_M[\ell + 2nM]z^{-n}$. We will also denote by \mathbf{P}_1 and \mathbf{P}_2 the $M \times \kappa$ matrices formed by selecting the M upper and lower rows of \mathbf{P} respectively, namely $\mathbf{P} = [\mathbf{P}_1^T, \mathbf{P}_2^T]^T$. The symmetry property $p_M[k] = p_M[N - k + 1]$ implies that $\mathbf{P}_1 = \mathbf{J}_M \mathbf{P}_2 \mathbf{J}_\kappa$, where \mathbf{J}_m is the $m \times m$ all-zero matrix with ones in the anti-diagonal.

Figures 1 and 2 respectively represent the polyphase network based implementations of the modulator and demodulator of the OFDM/OQAM signal, see [5] for further details. The input of the modulator are the real and imaginary parts of the original complex-valued symbols to be transmitted. More specifically, let us consider the transmission of N_s multicarrier symbols. The original $2M \times N_s$ complex-valued symbols are transformed into $2M \times 2N_s$ real-valued symbols, denoted as $a_k[n]$, $k = 1 \dots 2M$, $n = 0 \dots 2N_s - 1$, that contain their real and imaginary parts. These real-valued symbols are the input to the polyphase network in Figure 1, and are the ones that are detected at the output of the polyphase network in Figure 2, after the $\text{Re}[\cdot]$ function.

The first operation in the polyphase network of the modulator in Figure 1 consists in a multiplication of $a_k[n]$ by $\sqrt{2}j^n$, where j denotes the imaginary unit. As a consequence, $a_k[n]j^n$ will be real-valued for even n and purely imaginary for odd n . We will gather the n -even and n -odd samples into two different $2M \times N_s$ matrices, that will be denoted by \mathbf{B} and \mathbf{C} respectively. Note that \mathbf{B} contains real-valued values, whereas \mathbf{C} contains purely imaginary ones.

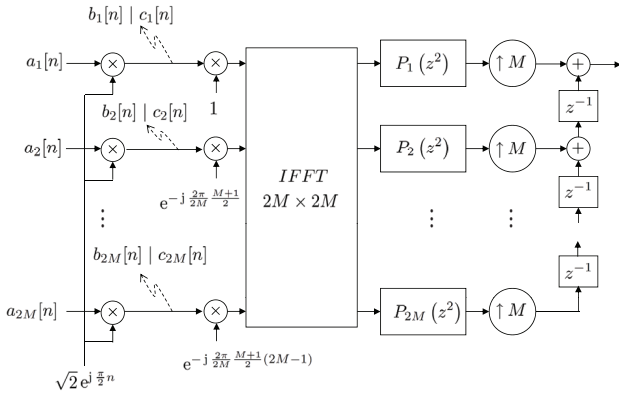


Fig. 1. Polyphase implementation of the OFDM/OQAM modulator.

2.1. Received signal with no frequency selectivity

Consider the signal $y_k[n]$ obtained in the polyphase reconstruction network, after the IFFT operation and right before the multiplication by the time factor $\sqrt{2}j^n$ (see further Figure 2). We can gather n -odd and n -even samples of $y_k[n]$

into two different $2M \times (N_s + 2\kappa)$ matrices \mathbf{Y}_1 and \mathbf{Y}_2 respectively. Since we are essentially considering here the case of frequency flat fading, and in order to differentiate the notation from the one obtained under frequency selectivity, we will add the superscript “ff” (frequency flat) to the matrices, i.e. $\mathbf{Y}_1^{(\text{ff})}$ and $\mathbf{Y}_2^{(\text{ff})}$. We will denote by \otimes the row-wise convolution of matrices, i.e. $\mathbf{U} \otimes \mathbf{V}$ is defined to be a matrix whose i th row is the convolution of the i th rows of \mathbf{U} and \mathbf{V} . After some tedious but simple algebraic manipulations we can express the matrices $\mathbf{Y}_1^{(\text{ff})}$ and $\mathbf{Y}_2^{(\text{ff})}$ as

$$\mathbf{Y}_1^{(\text{ff})} = 2\Phi \mathbf{F}_{2M}^H ([\mathbf{F}_{2M} \Phi^* \mathbf{B}, \mathbf{0}, \mathbf{0}] \otimes \mathcal{R}_{pp}) + 2\Phi \mathbf{F}_{2M}^H \left(\begin{bmatrix} \mathbf{0}, \mathbf{G}_2 \Phi^* \mathbf{C}, \mathbf{0} \\ \mathbf{G}_1 \Phi^* \mathbf{C}, \mathbf{0}, \mathbf{0} \end{bmatrix} \otimes \mathcal{S}_{pp} \right) \quad (2)$$

and

$$\mathbf{Y}_2^{(\text{ff})} = 2\Phi \mathbf{F}_{2M}^H ([\mathbf{0}, \mathbf{F}_{2M} \Phi^* \mathbf{C}, \mathbf{0}] \otimes \mathcal{R}_{pp}) + 2\Phi \mathbf{F}_{2M}^H \left(\begin{bmatrix} \mathbf{0}, \mathbf{G}_2 \Phi^* \mathbf{B}, \mathbf{0} \\ \mathbf{G}_1 \Phi^* \mathbf{B}, \mathbf{0}, \mathbf{0} \end{bmatrix} \otimes \mathcal{S}_{pp} \right) \quad (3)$$

respectively, where $\mathbf{0}$ is an all-zeros column vector of appropriate dimensions, $(\cdot)^*$ and $(\cdot)^H$ indicate complex conjugate and conjugate transpose respectively, \mathbf{F}_{2M} is the $2M \times 2M$ Fourier matrix

$$\{\mathbf{F}_{2M}\}_{1 \leq i, j \leq 2M} = \frac{1}{\sqrt{2M}} \exp \left(j \frac{2\pi}{2M} (i-1)(j-1) \right),$$

\mathbf{G}_1 (resp. \mathbf{G}_2) contains the M upper (resp. lower) rows of \mathbf{F}_{2M} respectively so that $\mathbf{F}_{2M} = [\mathbf{G}_1^T, \mathbf{G}_2^T]^T$, and where we have defined

$$\Phi = \text{diag}_{m=0 \dots 2M-1} \left\{ \exp \left[j \pi \frac{M+1}{2M} m \right] \right\}$$

$$\mathcal{R}_{pp} = \begin{bmatrix} \mathbf{P}_1 \otimes \mathbf{J}_M \mathbf{P}_2 \\ \mathbf{P}_2 \otimes \mathbf{J}_M \mathbf{P}_1 \end{bmatrix}, \quad \mathcal{S}_{pp} = \begin{bmatrix} \mathbf{P}_2 \otimes \mathbf{J}_M \mathbf{P}_2 \\ \mathbf{P}_1 \otimes \mathbf{J}_M \mathbf{P}_1 \end{bmatrix}.$$

In [5], a set of sufficient conditions are given on the discrete prototype pulse, which ensure perfect reconstruction of the transmitted symbols at the receiver. In our notation, this reconstruction condition can be expressed as follows:

$$\mathcal{R}_{pp} + (\mathbf{I}_2 \otimes \mathbf{J}_M) \mathcal{R}_{pp} = [\mathbf{0}_{2M \times (\kappa-1)} \quad \mathbf{1}_{2M \times 1} \quad \mathbf{0}_{2M \times (\kappa-1)}] \quad (4)$$

where $\mathbf{0}_{a \times b}$ (resp. $\mathbf{1}_{a \times b}$) is an $a \times b$ matrix with all zeros (resp. ones), \mathbf{I}_k is the $k \times k$ identity matrix and \otimes denotes Kronecker product. Indeed, observe that we can express the real part of \mathbf{Y}_1 as

$$\begin{aligned} \text{Re} \left[\mathbf{Y}_1^{(\text{ff})} \right] &= \frac{1}{2} \left(\mathbf{Y}_1^{(\text{ff})} + \left(\mathbf{Y}_1^{(\text{ff})} \right)^* \right) \\ &= \Phi \mathbf{F}_{2M}^H ([\mathbf{F}_{2M} \Phi^* \mathbf{B}, \mathbf{0}, \mathbf{0}] \otimes [\mathcal{R}_{pp} + (\mathbf{I}_2 \otimes \mathbf{J}_M) \mathcal{R}_{pp}]) + \\ &+ \Phi \mathbf{F}_{2M}^H \left(\begin{bmatrix} \mathbf{0}, \mathbf{G}_2 \Phi^* \mathbf{C}, \mathbf{0} \\ \mathbf{G}_1 \Phi^* \mathbf{C}, \mathbf{0}, \mathbf{0} \end{bmatrix} \otimes [\mathcal{S}_{pp} - (\mathbf{I}_2 \otimes \mathbf{J}_M) \mathcal{S}_{pp}] \right) \end{aligned}$$

where we have used the fact that $\mathbf{F}_{2M} = \mathbf{F}_{2M}^T$, $\mathbf{B}^* = \mathbf{B}$, $\mathbf{C}^* = -\mathbf{C}$, and also the identity $\Phi^* \mathbf{F}_{2M} = \Phi \mathbf{F}_{2M}^H (\mathbf{I}_2 \otimes \mathbf{J}_M)$. Noting that, by definition $(\mathbf{I}_2 \otimes \mathbf{J}_M) \mathcal{S}_{pp} = \mathcal{S}_{pp}$, we see that the second term of the above equation is zero. Imposing (4) we can readily conclude that

$$\text{Re} \left[\mathbf{Y}_1^{(\text{ff})} \right] = [\mathbf{0}_{2M \times \kappa-1}, \mathbf{B}, \mathbf{0}_{2M \times \kappa+1}] \quad (5)$$

and, quite similarly,

$$\text{Im} \left[\mathbf{Y}_2^{(\text{ff})} \right] = [\mathbf{0}_{2M \times \kappa}, \mathbf{C}, \mathbf{0}_{2M \times \kappa}]. \quad (6)$$

Hence, the perfect reconstruction condition in (4) guarantees that we can perfectly recover the transmitted symbols from $\text{Re} \left[\mathbf{Y}_1^{(\text{ff})} \right]$ and $\text{Im} \left[\mathbf{Y}_2^{(\text{ff})} \right]$. Unfortunately, the expressions of $\text{Im} \left[\mathbf{Y}_1^{(\text{ff})} \right]$ and $\text{Re} \left[\mathbf{Y}_2^{(\text{ff})} \right]$ do not accept such nice closed forms.

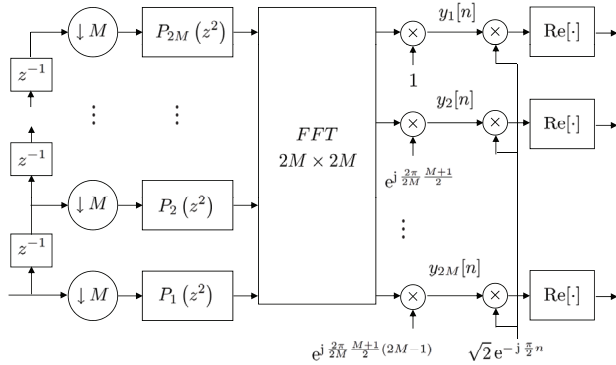


Fig. 2. Polyphase implementation of the OFDM/OQAM demodulator.

3. EFFECT OF CHANNEL FREQUENCY SELECTIVITY

We will next consider here the effect of a finite impulse response channel of length L_h and impulse response $h[\ell]$, $\ell = 0 \dots L_h - 1$. For simplicity, we will assume that $L_h < M$, which is quite reasonable in practical scenarios. Let \mathcal{C}_{2M} denote the $2M \times 2M$ unitary circular displacement matrix

$$\mathcal{C}_{2M} = \begin{bmatrix} 0 & 1 & 0 & 0 \\ \vdots & 0 & \ddots & 0 \\ 0 & \ddots & \ddots & 1 \\ 1 & 0 & \cdots & 0 \end{bmatrix}$$

and define \mathbb{H} as the circulant matrix $\mathbb{H} = \sum_{\ell=0}^{L_h-1} h[\ell] \mathcal{C}_{2M}^\ell$. We define $\mathbf{P}_1^{(\ell)}$, $\mathbf{P}_2^{(\ell)}$ as the matrices obtained from \mathbf{P}_1 and \mathbf{P}_2 after right-displacement by exactly one column of the entries

of the ℓ last rows of \mathbf{P}_1 and \mathbf{P}_2 respectively, that is in Matlab notation

$$\mathbf{P}_i^{(\ell)} = \begin{bmatrix} \mathbf{P}_i(1 : M - \ell, :), \mathbf{0} \\ \mathbf{0}, \mathbf{P}_i(M - \ell + 1 : M, :) \end{bmatrix}$$

with $i = 1, 2$. We also define

$$\mathcal{R}_{pp}(\ell) = \begin{bmatrix} \mathbf{P}_1 \\ \mathbf{P}_2^{(\ell)} \end{bmatrix} \otimes \mathcal{C}_{2M}^\ell \mathbf{J}_{2M} \begin{bmatrix} \mathbf{P}_1 \\ \mathbf{P}_2 \end{bmatrix}$$

$$\mathcal{S}_{pp}(\ell) = \begin{bmatrix} \mathbf{P}_2 \\ \mathbf{P}_1^{(\ell)} \end{bmatrix} \otimes \mathcal{C}_{2M}^\ell \begin{bmatrix} \mathbf{J}_M \mathbf{P}_2 \\ \mathbf{J}_M \mathbf{P}_1 \end{bmatrix}$$

and we point out that $\mathcal{R}_{pp}(0) = \mathcal{R}_{pp}$ and $\mathcal{S}_{pp}(0) = \mathcal{S}_{pp}$. Using the above definitions we can express the matrices \mathbf{Y}_1 and \mathbf{Y}_2 as it is shown at the top of the next page, with Θ_{2M} denoting a diagonal matrix defined as $\Theta_{2M} = \mathbf{F}_{2M} \mathcal{C}_{2M} \mathbf{F}_{2M}^H$, i.e. $\{\Theta_{2M}\}_{kk} = e^{-j \frac{2\pi}{2M} (k-1)}$. Due to the dependence of $\mathcal{R}_{pp}(\ell)$ and $\mathcal{S}_{pp}(\ell)$ on ℓ , it is not possible to decouple the effect of the channel frequency selectivity into a set of coefficients weighting the signal at each of the received carriers (as it the case in OFDM modulations). To formalize this, let us define Λ_H as the diagonal matrix that contains the FFT of the channel coefficients,

$$\Lambda_H = \mathbf{F}_{2M} \mathbb{H} \mathbf{F}_{2M}^H = \sum_{\ell=0}^{L_h-1} h[\ell] \Theta_{2M}^\ell$$

so that the k th diagonal entry of this matrix can be written as $\{\Lambda_H\}_{kk} = H\left(\frac{k-1}{2M}\right)$, where $H(\omega)$ is the Fourier transform of the channel impulse response. In practice, we would like to have $\mathbf{Y}_1 = \Lambda_H \mathbf{Y}_1^{(\text{ff})}$ and $\mathbf{Y}_2 = \Lambda_H \mathbf{Y}_2^{(\text{ff})}$ where here $\mathbf{Y}_i^{(\text{ff})}$, $i = 1, 2$ are defined in (2)-(3). Indeed, assuming that the receiver has perfect channel knowledge, we could recover \mathbf{B} and \mathbf{C} from $\text{Re} \left[\Lambda_H^{-1} \mathbf{Y}_1 \right]$ and $\text{Im} \left[\Lambda_H^{-1} \mathbf{Y}_2 \right]$ respectively as it was shown above, which means that single tap carrier-by-carrier equalization would be optimal. However, this is not the case due to the dependence of $\mathcal{R}_{pp}(\ell)$ and $\mathcal{S}_{pp}(\ell)$ on ℓ in the expressions of \mathbf{Y}_1 and \mathbf{Y}_2 obtained under frequency selective fading. This dependence causes inter-symbol and inter-carrier interference at the received samples, which cannot be compensated with single tap equalization.

4. CHARACTERIZATION OF THE INTER-SYMBOL AND INTER-CARRIER INTERFERENCE

It seems rather intuitive to think that both inter-symbol and inter-carrier interference of FBMC modulations disappear as the number of carriers increase without bound ($M \rightarrow \infty$). Here we make this statement a bit more precise and characterize the residual interference in this asymptotic regime. To that effect, we will assume that the prototype pulse is obtained by sampling a sufficiently smooth analog pulse, so that we can write

$$p_M[n] = p \left(\left(n - \frac{N+1}{2} \right) \frac{T_s}{2M} \right)$$

$$\begin{aligned}\mathbf{Y}_1 &= 2 \sum_{\ell=1}^{L_h-1} h[\ell] \Theta_{2M}^\ell \Phi \mathbf{F}_{2M}^H ([\mathbf{F}_{2M} \Phi^* \mathbf{B}, \mathbf{0}, \mathbf{0}] \otimes \mathcal{R}_{pp}(\ell)) + 2 \sum_{\ell=1}^{L_h-1} h[\ell] \Theta_{2M}^\ell \Phi \mathbf{F}_{2M}^H \left(\begin{bmatrix} \mathbf{0}, \mathbf{G}_2 \Phi^* \mathbf{C}, \mathbf{0} \\ \mathbf{G}_1 \Phi^* \mathbf{C}, \mathbf{0}, \mathbf{0} \end{bmatrix} \otimes \mathcal{S}_{pp}(\ell) \right) \\ \mathbf{Y}_2 &= 2 \sum_{\ell=1}^{L_h-1} h[\ell] \Theta_{2M}^\ell \Phi \mathbf{F}_{2M}^H ([\mathbf{0}, \mathbf{F}_{2M} \Phi^* \mathbf{C}, \mathbf{0}] \otimes \mathcal{R}_{pp}(\ell)) + 2 \sum_{\ell=1}^{L_h-1} h[\ell] \Theta_{2M}^\ell \Phi \mathbf{F}_{2M}^H \left(\begin{bmatrix} \mathbf{0}, \mathbf{G}_2 \Phi^* \mathbf{B}, \mathbf{0} \\ \mathbf{G}_1 \Phi^* \mathbf{B}, \mathbf{0}, \mathbf{0} \end{bmatrix} \otimes \mathcal{S}_{pp}(\ell) \right)\end{aligned}$$

for $n = 1 \dots N$, where $p(t)$ is an analog waveform independent of M and T_s is the multicarrier symbol period in seconds (equivalent to the duration of $2M$ samples). We will assume that $p(t)$ is twice continuously differentiable with bounded derivatives and we will define

$$d_M[n] = T_s p' \left(\left(n - \frac{N+1}{2} \right) \frac{T_s}{2M} \right)$$

where $p'(t)$ its the first derivative of $p(t)$. By using the Taylor expansion of $p(t)$ around the n th sampling instant, we can write (as $M \rightarrow \infty$)

$$p_M[n + \ell] = p_M[n] + \frac{\ell}{2M} d_M[n] + \mathcal{O} \left(\frac{1}{M^2} \right).$$

Using this we can approximate the entries of $\mathcal{R}_{pp}(\ell)$ and $\mathcal{S}_{pp}(\ell)$ as²

$$\begin{aligned}\mathcal{R}_{pp}(\ell) &= \mathcal{R}_{pp} - \frac{\ell}{2M} \mathcal{R}_{pd} + \mathcal{O} \left(\frac{1}{M^2} \right) \\ \mathcal{S}_{pp}(\ell) &= \mathcal{S}_{pp} - \frac{\ell}{2M} \mathcal{S}_{pd} + \mathcal{O} \left(\frac{1}{M^2} \right)\end{aligned}$$

where we have defined

$$\mathcal{R}_{pd} = \begin{bmatrix} \mathbf{P}_1 \otimes \mathbf{J}_M \mathbf{D}_2 \\ \mathbf{P}_2 \otimes \mathbf{J}_M \mathbf{D}_1 \end{bmatrix} \quad \mathcal{S}_{pd} = \begin{bmatrix} \mathbf{P}_2 \otimes \mathbf{J}_M \mathbf{D}_2 \\ \mathbf{P}_1 \otimes \mathbf{J}_M \mathbf{D}_1 \end{bmatrix}$$

with \mathbf{D}_1 (resp. \mathbf{D}_2) being defined as the $M \times \kappa$ matrix obtained by selecting the M upper (resp. lower) rows of \mathbf{D} , which is in turn defined as \mathbf{P} in (1) but replacing the pulse samples $p_M[n]$ by the samples of its derivative $d_M[n]$.

Now, assuming that the entries in \mathbf{B} and \mathbf{C} are bounded (as it is the case if the symbols are taken from a fixed constellation independent of M), we will be able to write

$$\mathbf{Y}_1 = \Lambda_H \mathbf{Y}_1^{(\text{ff})} - j \frac{1}{2M} \Lambda_D \tilde{\mathbf{Y}}_1 + \mathcal{O} \left(\frac{1}{M^2} \right) \quad (7)$$

$$\mathbf{Y}_2 = \Lambda_H \mathbf{Y}_2^{(\text{ff})} - j \frac{1}{2M} \Lambda_D \tilde{\mathbf{Y}}_2 + \mathcal{O} \left(\frac{1}{M^2} \right) \quad (8)$$

where $\tilde{\mathbf{Y}}_1$ (resp. $\tilde{\mathbf{Y}}_2$) is defined as $\mathbf{Y}_1^{(\text{ff})}$ (resp. $\mathbf{Y}_2^{(\text{ff})}$) by replacing \mathcal{R}_{pp} and \mathcal{S}_{pp} by the above-introduced quantities \mathcal{R}_{pd} and \mathcal{S}_{pd} respectively. Furthermore, in the above equations we have defined Λ_D as a diagonal matrix containing the derivatives of the channel frequency response, i.e. $\Lambda_D = -j \sum_{\ell=1}^{L_h-1} \ell h[\ell] \Theta_{2M}^\ell$ so that the k th diagonal entry can be expressed as $\{\Lambda_D\}_{kk} = H' \left(\frac{k-1}{2M} \right)$ with $H'(\omega)$ denoting the first derivative of $H(\omega)$.

We can readily observe from the asymptotic expressions of \mathbf{Y}_1 and \mathbf{Y}_2 in (7) and (8) that a single tap carrier-by-carrier equalizer is only optimal when $M \rightarrow \infty$. For moderate values of M , the first order error terms $\tilde{\mathbf{Y}}_1$ and $\tilde{\mathbf{Y}}_2$ will be the main cause of distortion in terms of both inter-symbol and inter-carrier interference. Indeed, observe that by taking the real and imaginary parts of the samples after the single-tap carrier-by-carrier equalizer, we will have

$$\begin{aligned}\text{Re} [\Lambda_H^{-1} \mathbf{Y}_1] &= \text{Re} [\mathbf{Y}_1^{(\text{ff})}] - \frac{1}{2M} \mathbf{E}_1 + \mathcal{O} \left(\frac{1}{M^2} \right) \\ \text{Im} [\Lambda_H^{-1} \mathbf{Y}_2] &= \text{Im} [\mathbf{Y}_2^{(\text{ff})}] - \frac{1}{2M} \mathbf{E}_2 + \mathcal{O} \left(\frac{1}{M^2} \right)\end{aligned}$$

where $\mathbf{E}_1 = \text{Im} [\Lambda_H^{-1} \Lambda_D \tilde{\mathbf{Y}}_1]$ and $\mathbf{E}_2 = \text{Re} [\Lambda_H^{-1} \Lambda_D \tilde{\mathbf{Y}}_2]$ are the two first-order distortion terms.

In order to determine the average level of distortion at the output of the filterbank receiver, it is useful to consider the transmitted symbols as independent and identically distributed (i.i.d.) random quantities, so that \mathbf{E}_1 and \mathbf{E}_2 are also random. More specifically, we will model the entries of \mathbf{B} and \mathbf{C} as i.i.d. random variables with zero mean and power σ_b^2 and σ_c^2 respectively. Under these assumptions, the (k, ℓ) th entries of \mathbf{E}_1 and \mathbf{E}_2 will also have zero mean. Furthermore, if ℓ is chosen so that tail effects are disregarded (i.e. $2\kappa \leq \ell \leq N_s - 2\kappa$), we can write

$$\begin{aligned}\mathbb{E} [\{\mathbf{E}_1\}_{k,\ell}^2] &= \text{Re}^2 \{ \Lambda_H^{-1} \Lambda_D \}_{kk} \frac{\sigma_b^2}{M} \text{tr} (\mathbf{U}^- \mathcal{R}_{pd} \mathcal{R}_{pd}^T) \\ &\quad + \text{Im}^2 \{ \Lambda_H^{-1} \Lambda_D \}_{kk} \frac{\sigma_b^2}{M} \text{tr} (\mathbf{U}^+ \mathcal{R}_{pd} \mathcal{R}_{pd}^T) \\ &\quad + \text{Re}^2 \{ \Lambda_H^{-1} \Lambda_D \}_{kk} \frac{1}{M} \sigma_c^2 \text{tr} (\mathbf{U}^+ \mathcal{S}_{pd} \mathcal{S}_{pd}^T) \\ &\quad + \text{Im}^2 \{ \Lambda_H^{-1} \Lambda_D \}_{kk} \frac{\sigma_c^2}{M} \text{tr} (\mathbf{U}^- \mathcal{S}_{pd} \mathcal{S}_{pd}^T) \quad (9)\end{aligned}$$

²In the following, the symbol $\mathcal{O}(M^{-2})$ is used to denote a matrix (with dimensions potentially increasing with M) whose entries decay as M^{-2} .

where $\mathbf{U}^+ = \mathbf{I}_2 \otimes (\mathbf{I}_M + \mathbf{J}_M)$ and $\mathbf{U}^- = \mathbf{I}_2 \otimes (\mathbf{I}_M - \mathbf{J}_M)$. The expression of $\mathbb{E} \left[\{\mathbf{E}_2\}_{k,\ell}^2 \right]$ can be found to be exactly the same but swapping the role of σ_b^2 and σ_c^2 .

It is worth pointing out that the asymptotic MSE of the residual distortion after a frequency non-selective channel presents a nontrivial dependence on the correlation between the polyphase components of pulse prototype and the polyphase components of its derivative. Furthermore, the residual distortion has a direct relationship with the degree of variation (relative derivative) of the channel frequency response, which seems rather intuitive.

5. SIMULATIONS

We considered an OFDM/OQAM system with $2M = 256$ carriers using a prototype pulse constructed from sampling a Nyquist square root raised cosine pulse (roll-off 100%) truncated to $\kappa = 8$ symbol periods. This pulse does not exactly meet the reconstruction constraints in (4) but this is not important for the purposes of evaluating the average distortion at the output of the receiving filterbank (we do not consider here the degradation produced by the pulse and assume that the equations (5)-(6) hold true). The symbols $a_k[n]$ were independently drawn from the real and imaginary parts of a 16-QAM modulation with total unit power, and the noiseless channel was randomly generated according to an exponential power delay profile and presented the frequency response shown in the upper plot of Figure 3. The lower plot shows the average signal to distortion ratio (SDR) of the real/imaginary parts of the equalized signal (after single tap carrier-by-carrier equalization), which is defined as the quotient between the signal power and the average MSE of the signal with respect to $\mathbf{Y}_i^{(ff)}$, $i = 1, 2$. We also represent the SDR predicted by the average asymptotic distortion power in (9).

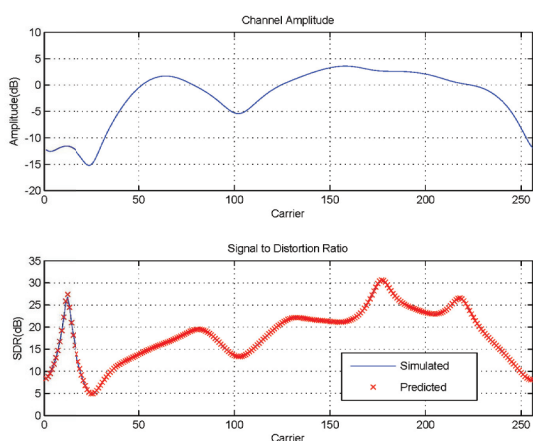


Fig. 3. Comparison between true and averaged asymptotic distortion for the channel response in the upper plot.

Observe first that the predicted error distortion is almost identical to the simulated one, even for a situation where the number of carriers is not excessively large (current OFDM systems implement a number of carriers that is at least an order of magnitude higher). This confirms the usefulness of the derived expressions in order to determine the performance of the global OFDM/OQAM system. On the other hand, it is also interesting to notice that a low channel response at a particular carrier does not necessarily imply that the corresponding distortion should be high. As it was predicted in (9) inter-symbol and inter-carrier interference only increase when the channel frequency response shows high relative variations.

6. CONCLUSIONS

We have characterized the distortion caused by inter-symbol and inter-carrier interference of an OFDM/OQAM system under a frequency selective channel. The approach is asymptotic in the number of carriers (M), but it provides a very good approximation for the typical values M used in typical commercial communication systems. The residual distortion caused by the channel frequency selectivity depends critically on the relative derivative of the channel frequency response, as well as on the cross-correlation between the polyphase components of the prototype pulse and those of its derivative.

7. REFERENCES

- [1] B. L. Floch, M. Alard, and C. Berrou, "Coded orthogonal frequency division multiplex," *Proceedings of the IEEE*, vol. 83, pp. 982 – 996, 1995.
- [2] T. Ihalainen, T. H. Stitz, M. Rinne, and M. Renfors, "Channel equalization in filter bank based multicarrier modulation for wireless communications," *EURASIP Journal on Advances in Signal Processing*, vol. 2007, pp. 1–18, 2007.
- [3] H. Lin, C. Lele, and P. Siohan, "Equalization with interference cancellation for hermitian symmetric OFDM/OQAM systems," in *Proceedings of the IEEE IS-PLC 2008.*, pp. 363 – 368.
- [4] L. Baltar, D. Waldhauser, and J. Nossek, "MMSE sub-channel decision feedback equalization for filter bank based multicarrier systems," in *Proceedings of the IEEE ISCAS 2009.*, 2009, pp. 2802 – 2805.
- [5] P. Siohan, C. Siclet, and N. Lacaille, "Analysis and design of OFDM/OQAM systems based on filterbank theory," *IEEE Transactions on Signal Processing*, vol. 50, no. 5, pp. 1170–1183, May 5.